Inhibition of Monoamine Oxidase-B by Condensed Pyridazines and Pyrimidines: Effects of Lipophilicity and Structure−Activity Relationships

Cosimo Altomare, Saverio Cellamare, Luciana Summo, Marco Catto, and Angelo Carotti*

Dipartimento Farmaco-chimico, Università di Bari, Via Orabona 4, I-70125 Bari, Italy

Ulrike Thull, Pierre-Alain Carrupt, and Bernard Testa

Institut de Chimie Thérapeutique, Section de Pharmacie, Université de Lausanne, CH-1015 Lausanne-Dorigny, Switzerland

Helen Stoeckli-Evans

Institut de Chimie, Faculté de Sciences, Université de Neuchâtel, Avenue de Bellevaux 51, CH-2000 Neuchâtel, Switzerland

Received February 23, 1998

A number of condensed pyridazines and pyrimidines were synthesized and tested for their monoamine oxidase-A (MAO-A) and MAO-B inhibitory activity. Their lipophilicity was examined by measuring partition coefficients and RP-HPLC capacity factors, revealing some peculiar electronic and conformational effects. Further insights were obtained by X-ray crystallography and a thermodynamic study of RP-HPLC retention. Structure−activity relations highlighted the main factors determining both selectivity and inhibitory potency. Thus, while most of the condensed pyridazines were reversible inhibitors of MAO-B with little or no MAO-A effects, the pyrimidine derivatives proved to be reversible and selective MAO-A inhibitors. Substituents on the diazine nucleus modulated enzyme inhibition. A QSAR analysis of X-substituted 3-X-phenyl-5*H*-indeno[1,2-*c*]pyridazin-5-ones showed lipophilicity to increase MAO-B and not MAO-A inhibitory activity.

Introduction

Monoamine oxidase (MAO, EC 1.4.3.4) is a FAD-containing enzyme of the outer mitochondrial membrane that catalyzes the oxidative deamination of various neurotransmitters and dietary amines.[1] MAO exists in two enzymatic forms termed MAO-A and MAO-B and differing by their substrate specificity, sensitivity to inhibitors,[2] and amino acid sequence.[3] MAO-A and MAO-B have 70% sequence identity and have been expressed from two genes with similar structures. Their three-dimensional structures are not known, but recently, relevant information about their active site has been reported.[4] In recent years, there has been a considerable renewal of interest in MAO for two main reasons. One was the discovery that the neurotoxin 1-methyl-4-phenyl-1,2,3,6-tetrahydropyridine (MPTP) causes the death of dopaminergic neurons and induces symptoms very similar to Parkinson's disease in humans.[5] The second reason was the observation that selective and reversible inhibitors of MAO-A or MAO-B may be useful therapeutic agents devoid of undesirable side-effects such as hypertensive crises and cardiac arrhythmias caused by the alimentary intake of tyramine.[6] In humans, MAO-B inhibitors (e.g., deprenyl) are useful as coadjuvants in the treatment of Parkinson's disease and perhaps Alzheimer's disease,[7] whereas MAO-A inhibitors are valuable antidepressant and antianxiety agents (e.g., moclobemide).[8]

In previous papers, we examined the MAO-mediated toxication of MPTP analogues[9] and the MAO inhibitory activity of isoquinoline derivatives[10] and condensed pyridazines.[11] Thus, we described 5*H*-indeno[1,2-*c*]-pyridazin-5-ones, hereafter termed IPyd, some of which were found to be reversible and competitive inhibitors of MAO-B with little or no effect on MAO-A. A lead optimization study by means of QSAR led to a predictive 3D-QSAR model and to the design of 3-*p*-CF_3-phenyl-IPyd derivatives showing submicromolar inhibition values toward MAO-B (IC_{50} = 90 nM). The influence of lipophilicity in increasing inhibition of MAO-B (but not MAO-A) was demonstrated by a traditional QSAR Hansch-type analysis and by a comparative molecular field analysis (CoMFA) including the molecular lipophilicity potential (MLP).[12]

To deepen our understanding of the MAO inhibitory activity and selectivity of diazine-containing compounds,

Table 1. MAO Inhibition Data of Newly Synthesized Pyridazine and Pyrimidine Derivatives

	IC_{50} (μM) or % inhibition at μM[b]	
compd no.	MAO-A	MAO-B
1	18% at 100	29% at 100
2	97.6 ± 8.9	27.5 ± 5.1
7	0% at 25	21.0 ± 0.6
26	44% at 50	12% at 50
29	59.1 ± 2.7	74.8 ± 9.7
30	16.4 ± 3.0	32% at 125
31	15% at 5	12.5% at 5
32	0% at 5	0% at 5
35	2.37 ±0.11	11.6 ± 1.1
36	8.39 ± 0.57	28% at 10

[a] The inhibitory activity values of 5*H*-indeno[1,2-*c*]pyridazin-5-one derivatives **2** and **7** taken from ref 11 are reported as references. [b] Maximum solubility.

* Corresponding author. Fax: ++39.80.5442724. E-mail: carotti@farmchim.uniba.it.

S0022-2623(98)01005-X CCC: $15.00
Published on Web 09/04/1998

Table 2. Partition Coefficients and Themodynamic Parameters of RP-HPLC Retention of Pyridazine and Pyrimidine Derivatives

compd				partition data[b]			RP-HPLC retention data		
no.	R_3	R_4	pIC_{50} (MAO-B)	CLOG *P*	log P_{oct}	log P_{cyh}	log k^f	$\Delta H°$ (kJ/mol)[g]	$[\Delta S°/R + \ln \phi]$[g]
1				1.05	1.09	−0.45	−0.04	−3.99 (0.22)	−2.6 (0.2)
2	H	H	4.56	1.13	1.22	−0.29	0.03	−13.5 (0.7)	−3.3 (0.3)
3	CH_3	H	4.12	1.63	1.58	−0.04	0.46	−6.27 (0.37)	−1.4 (0.1)
4	CF_3	H		2.03	2.21	0.70	0.74	−6.11 (0.33)	−1.3 (0.1)
5	H	Ph	4.03	3.02	2.80	1.40	1.22	−14.2 (1.3)	−2.8 (0.5)
6	Ph	CH_3		3.73	*c*	2.16	1.53	−15.1 (1.6)	−2.4 (0.6)
7	Ph	H	4.68	3.23	*c*	2.34	1.39	−7.1 (1.5)	−3.5 (0.6)
8	2′-NO_2−C_6H_4	H	4.10	2.98	2.64	1.05	0.93	−10.9 (1.2)	−2.1 (0.5)
9	3′-NO_2−C_6H_4	H	(6.2)[a]	2.98	*c*	1.66	1.35	−19.3 (1.7)	−4.5 (0.7)
10	4′-NO_2−C_6H_4	H	6.30	2.98	*c*	2.34	1.37	−19.0 (1.6)	−4.3 (0.6)
11	2′-OH−C_6H_4	H		2.60	*d*	2.55	1.51	−20.1 (0.2)	−4.4 (0.1)
12	4′-OH−C_6H_4	H	5.00	2.87	2.88	0.13	1.01	−19.7 (0.1)	−5.4 (0.1)
13	3′-NH_2−C_6H_4	H	4.49	2.29			0.79	−9.80 (1.25)	−2.0 (0.2)
14	4′-NH_2−C_6H_4	H	4.61	2.29			0.78	−19.0 (1.4)	−5.6 (0.7)
15	2′-OCH_3−C_6H_4	H		2.73	*c*	2.26	1.44	−16.3 (0.4)	−3.1 (0.2)
16	3′-OCH_3−C_6H_4	H	5.80	3.29	*c*	2.83	1.53	−19.5 (0.3)	−4.1 (0.1)
17	4′-OCH_3−C_6H_4	H	5.49	3.29	*c*	2.51	1.53	−20.8 (0.3)	−4.6 (0.1)
18	2′-F−C_6H_4	H	4.74	3.17	*c*	2.07	1.42	−15.5 (1.2)	−2.8 (0.4)
19	4′-F−C_6H_4	H	6.04	3.37	*c*	2.56	1.42	−15.0 (1.0)	−2.6 (0.3)
20	2′-Cl−C_6H_4	H	4.80	3.69			1.47	−11.8 (1.2)	−1.2 (0.3)
21	4′-Cl−C_6H_4	H	6.04	3.94			1.79	−19.9 (1.0)	−3.7 (0.4)
22	2′-CF_3−C_6H_4	H		4.11			1.52	−14.9 (0.6)	−2.3 (0.2)
23	4′-CF_3−C_6H_4	H	7.05	4.11			1.97	−19.5 (0.9)	−3.1 (0.3)
26				2.46			0.60	−5.83 (0.29)	−1.5 (0.1)
29			4.13	2.09	2.05	0.60	0.56	−8.83 (0.61)	−2.2 (0.1)
30				1.35	1.56	−2.22[e]	0.54	−15.5 (0.9)	−4.6 (0.4)
31				2.24			1.11	−24.9 (1.6)	−7.2 (0.6)
36			4.94	3.07	*c*	*c*	1.56	−16.2 (0.8)	−2.8 (0.2)
37				3.28	*c*	*c*	2.04	−20.5 (1.2)	−3.3 (0.4)

[a] Approximated value; 42% inhibition at 0.5 μM. [b] Partition coefficients are the means of at least 5 determinations (SD < 0.05 log units). [c] log *P* > 3.00. [d] log *P* = 3.15 ± 0.10. [e] Strong dependence of log P_{cyh} on solute concentration; −2.22 is the log *P* value extrapolated at infinite dilution. [f] Values are log of the capacity factor determined at the harmonic mean temperature (33 °C). [g] The standard errors are indicated in parentheses.

Scheme 1[a]

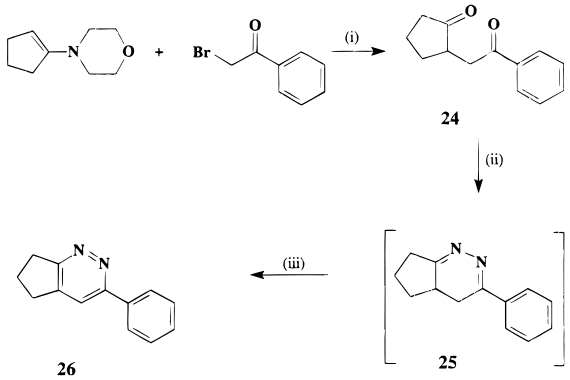

[a] Reagents: (i) dioxane, reflux; (ii) $NH_2NH_2 \cdot H_2O$; (iii) air oxidation, spontaneous.

Scheme 2[a]

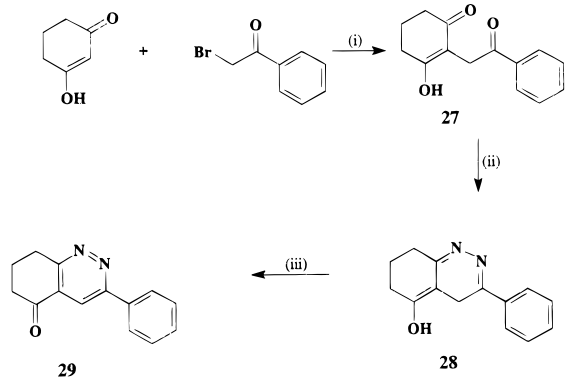

[a] Reagents: (i) KOH, MeOH; (ii) $NH_2NH_2 \cdot H_2O$, EtOH; (iii) DDQ, reflux.

drastic structural modifications of the lead compound (compound **7**, Table 2) were performed, yielding the structure−activity relationships presented here. The lipophilicity of various derivatives was also investigated, and new QSAR models of MAO-B inhibition were derived.

Results and Discussion

Chemistry. By replacing the condensed indane ring of 3-phenyl-5*H*-indeno[1,2-*c*]pyridazin-5-ones by other less hydrophobic rings and the pyridazine ring by a pyrimidine, novel compounds were obtained whose syntheses are outlined in Schemes 1−4.

4-Benzoylpyridazine **1** was prepared according to known procedures.[13] The cyclopenta[*c*]pyridazine derivative **26** was prepared as shown in Scheme 1. Treatment of the intermediate 2-phenacylcyclopentanone **24**, obtained from the reaction of ω-bromoacetophenone with 4-(1-cyclopenten-1-yl)morpholine in refluxing dry dioxane, with hydrazine hydrate gave **25**, which spontaneously dehydrogenated to compound **26**. Scheme 2 illustrates the synthesis of the tetrahydrocynnolinone derivative **29**. The intermediate product **27**, prepared according to a published method,[14] was treated with hydrazine hydrate to give compound **28** which was subsequently oxidized with DDQ to afford compound **29** in good yield.

The preparation of 3-phenyl-5,6,7,8-tetrahydro-pyrimido[4,5-*c*]pyridazin-5,7-dione **30** and its 4′-CF_3 congener **31**, hereafter called Pym-Pydones, was carried out by a one-pot procedure[11] as shown in Scheme 3. 3-Phenyl-5*H*-pyridazino[4,3-*b*]indole **32** was kindly made avail-

Scheme 3[a]

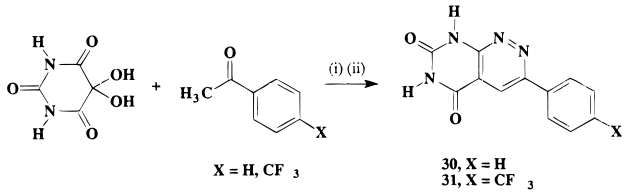

[a] Reagents: (i) HOAc, reflux; (ii) $NH_2NH_2 \cdot H_2O$.

able to us by Prof. F. Campagna (University of Bari, Italy) and was also investigated.

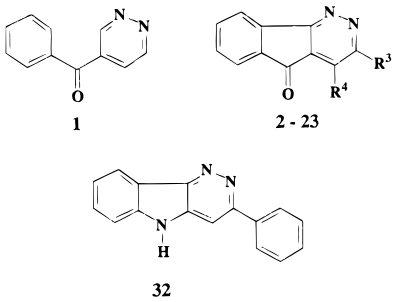

The syntheses of the indenopyrimidine derivatives **35** and **36** were accomplished in a three-step procedure as reported in Scheme 4. First, the enaminone intermediates **33a** and **33b** were prepared by reacting the appropriate indanone with *N*,*N*-dimethylformamide dimethyl acetal at room temperature and then reacted with benzamidine in refluxing dry ethanol to give the indenopyrimidines **34a**−**b** in very high yields. Finally, oxidation of compounds **34a**−**b** with CrO_3 afforded the desired 2-phenyl-9*H*-indeno[2,1-*d*]pyrimidin-9-one **35** and 2-phenyl-5*H*-indeno[1,2-*d*]pyrimidin-5-one **36**, respectively. All of the other compounds reported in Table 2 were prepared according to published procedures.[11,15]

Structure−**Lipophilicity Relations.** Lipophilicities of the diazine MAO inhibitors were assessed by measuring their 1-octanol/water (log P_{oct}) and cyclohexane/water (log P_{cyh}) partition coefficients and capacity factors (log *k*) in RP-HPLC (Table 2). Due to the limited precision of log *P* measurement of highly lipophilic compounds, only experimental log *P* values ≤3 were retained in structure−lipophilicity relationship studies. The values of log P_{oct} were also calculated by the CLOGP[16] algorithm. A good linear correlation was found between experimental and calculated log P_{oct} values ($r^2 = 0.957$). However, the CLOGP program[17] failed to predict some significant differences between positional isomers, which might be of interest in explaining variations in MAO inhibitory activity.

This is exemplified by the partitioning behavior of 3-(2′-OH-Ph) IPyd, which is much more lipophilic than 3-(4′-OH-Ph) IPyd (**11** and **12**, respectively) in the cyclohexane/water system. This difference is explained by the ability of the OH group, when in the ortho position of the phenyl group, to form an intramolecular H-bond (−OH···N═) with the pyridazine N(2), as demonstrated by the ^{1}H NMR chemical shifts of phenolic protons in $CDCl_3$ solvent (13.50 and 5.23 ppm for the *o*-OH, **11**, and *p*-OH, **12**, congeners, respectively). Completely unexpected was also the behavior of the *o*-NO_2 derivative **8**, which was markedly more hydrophilic than both its *m*- **9** and *p*-NO_2 **10** congeners, the differences

Scheme 4[a]

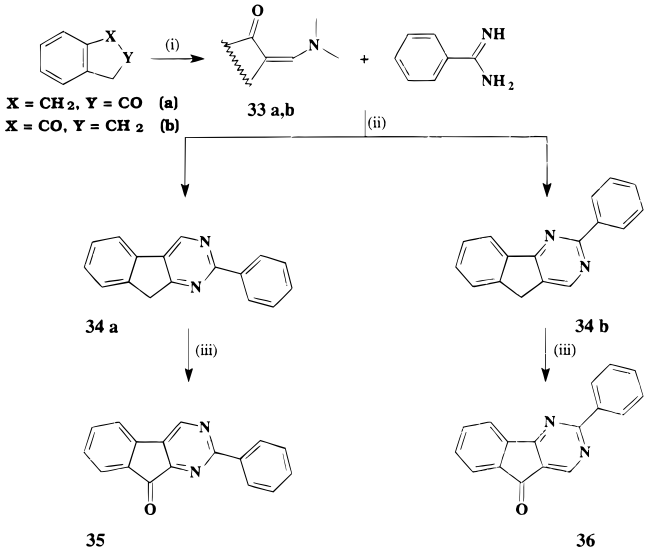

[a] Reagents: (i) $(CH_3)_2NCH(OCH_3)_2$, $CHCl_3$; (ii) NaOH in anhydrous EtOH, reflux; (iii) CrO_3, HOAc.

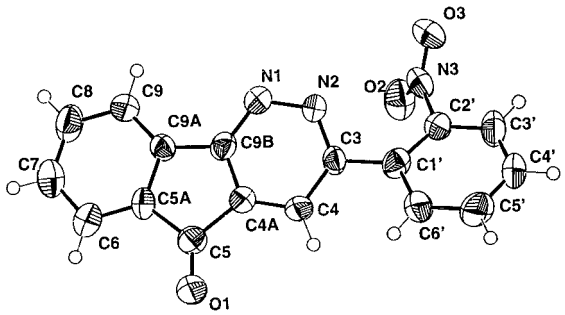

Figure 1. Perspective view of molecule **8** showing the numbering scheme used (thermal ellipsoids at 50% probability level).

in log *P* values being in the range 0.6−1.3 log *P* units. The strong increase of lipophilicity of the *m*- and *p*-nitrophenyl congeners could partly explain their relatively high MAO-B inhibitory activities.

The low lipophilicity of the *o*-nitro congener **8** could result from both conformational and electronic effects, all of which could be of enzymatic relevance. Indeed, loss of coplanarity between the NO_2 group and the phenyl ring and between the phenyl and the condensed pyridazine rings would decrease electronic conjugation and hence lipophilicity. To validate this hypothesis, the X-ray crystal structure of compound **8** was determined (Figure 1). The three fused rings of the indeno[1,2-*c*]-pyridazine moiety proved relatively planar. The nitrophenyl ring was staggered by 26.0(4)° relative to the pyridazine ring, and the dihedral angles between the NO_2 group and the phenyl and pyridazine rings were 61.6(5)° and 56.4(6)°, respectively. These torsion angles indicate a large deviation from planarity of the nitro group and may indeed account for the low lipophilicity of the compound.

As for the pyrimido[4,5-*c*]pyridazin-5,7-dione derivative **30**, its experimental log P_{oct} value (1.56) is very close to that calculated for the keto tautomer (1.35) rather than that for the enol tautomer (2.60), indicating a predominance of the former in solution.[18]

To obtain a more complete set of lipophilicity parameters, we also measured capacity factors (log *k* values)

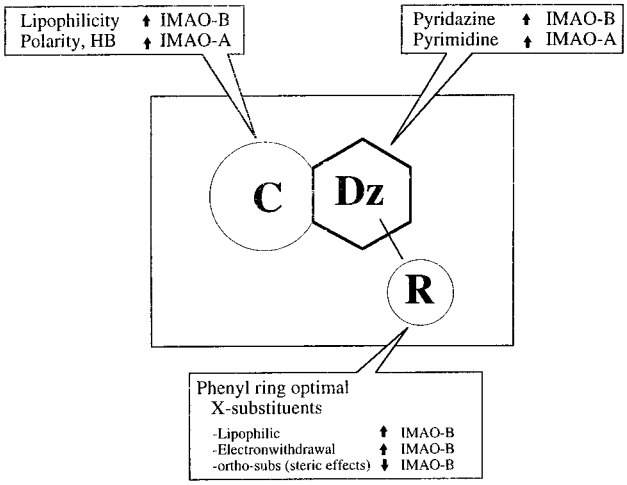

Figure 2. Summary of the main structural factors responsible for MAO I activity and MAO-A/B selectivity of pyridazine- and pyrimidine-containing derivatives. **Dz** = diazine ring; **C** = condensed ring; **R** = substituents on the diazine ring.

in RP-HPLC (Table 2). The influence of temperature on the RP-HPLC retention was also examined, leading to the enthalpy and entropy terms to be used below as thermodynamic parameters of lipophilicity in a QSAR analysis of MAO-B inhibition (Table 2). The distribution constant (K) of a solute between the stationary phase and mobile phase in a chromatographic system is a function of the difference in free energy of the solute in the two phases, $\Delta G°$[19]

$$RT \ln K = -\Delta G° = -(\Delta H° - T\Delta S°) \qquad (1)$$

where R is the gas constant and T is the absolute temperature. Substituting K with k/ϕ (ϕ being the phase ratio) yields a form of the van't Hoff equation

$$\ln k = -(\Delta H°/RT) + (\Delta S°/R) + \ln \phi \qquad (2)$$

Van't Hoff plots were constructed for each diazine derivative by collecting retention data in 5 °C increments from 18 to 48 °C. In all cases retention decreased with increasing temperature, indicating $\Delta H°$ to be negative and essentially independent from temperature in the explored range. Because the intercept includes a constant term dependent on the phase ratio and not known accurately, it was not possible to obtain reliable estimates for the magnitude of the entropic forces. Analysis can be made, however, in terms of group contributions to $\Delta S°$ (see below). Table 2 summarizes the data for the enthalpy and the entropy/phase ratio [$\Delta S°/R + \ln \phi$] terms (eq 2).

All data in Table 2 were examined for enthalpy−entropy compensation,[20] as shown in Figure 3. Such a compensation was found to exist for all IPyd derivatives except for the p-OH and p-NH_2 substituted congeners of 3-Ph IPyd, which showed a deviant behavior and were excluded from the regression. The compensation plot indicated that a single retention mechanism and similar solvation characteristics prevailed for most IPyd derivatives. Strong H-bond donors such as the Pym-Pydones (**30** and **31**) and the p-OH and p-NH_2 substituted 3-Ph IPyd were found to lie on an almost parallel line, indicating different solvation characteristics.

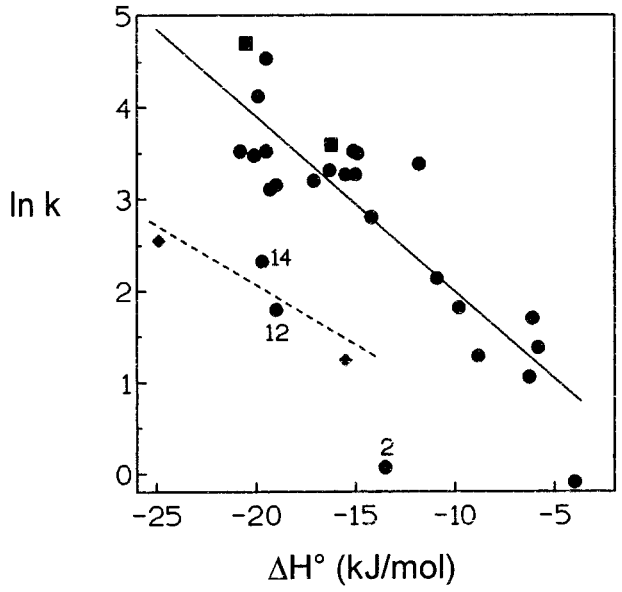

Figure 3. Enthalpy−entropy compensation plot showing capacity ratio, ln k, vs enthalpy, $\Delta H°$ (kJ mol^{-1}), found at the experimental harmonic mean temperature (33 °C) for RP-18 stationary phase and methanol/water (45/55, v/v) mobile phase: ●, IPyd; ■, IPym; ◆, Pym−Pydone. Drawn line is the regression line for IPyd congeners (**12** and **14** omitted as outliers).

MAO Inhibition. The newly synthesized compounds (**1**, **26**, **29**, **30**−**32**, **35**, and **36**) were tested for their inhibitory effect on MAO-A and MAO-B using a previously described method.[10,11,21] The IC_{50} values are reported in Table 1. The competitive, reversible MAO inhibitor harman was used as a reference for the two isozymes.[22] Preliminary measurements showed that all the tested compounds acted in a reversible and time-independent manner (results not shown).

No novel compound described here was more active than previously examined compounds. Nevertheless, the inhibition data in Table 1 give helpful information on structure−activity-selectivity relationships. For instance, a comparison between compounds **1** and **2** shows that rigidity and planarity should be favorable to activity, since 4-benzoylpyridazine **1** is about 4 times less active than 5*H*-indeno[1,2-*c*]pyridazin-5-one **2**. Furthermore, compounds **26**, **29**, **30**−**32**, and **7** indicate that the nature of the ring(s) condensed with pyridazine influenced activity and selectivity toward MAO-A. Indeed, replacing the indane ring with a cyclohexane or pyrimidine ring gave compounds **29** and **30**, respectively, which had marked MAO-A inhibitory activity. The pyrimido[4,5-*c*]pyridazine derivative **30** had the highest MAO-A inhibitory activity among all pyridazine-containing compounds tested so far in our laboratories. 3-Phenyl-5*H*-pyridazino[4,3-*b*]indole **32** did not show any detectable activity up to its maximum solubility.

The effect of diazine ring activity was explored by replacing the pyridazine with a pyrimidine ring. Indenopyrimidinones, termed IPym **35** and **36**, proved to be reversible inhibitors of MAO-B almost equipotent to the pyridazine analogue **7**, but with an additional and significant inhibitory activity toward MAO-A. 2-Phenyl-9*H*-indeno[2,1-*d*]pyrimidin-9-one **36** was the most active (IC_{50} = 2.37 μM) and selective analogue. This suggests that a diazine ring can influence both inhibitory potency

Table 3. Lipophilic Constants and Other Physicochemical Parameters of Substituents on 3-(X-Phenyl)-5*H*-indeno[1,2-*c*]pyridazin-5-one Used in QSAR Analysis of MAO-B Inhibition Data

compd no.	X	π	τ	τ_H	τ_S	σ	$V_{W(2')}$
7	H	0	0	0	0	0	0.08
8	2′-NO_2	−0.25	−0.46	−1.06	0.60	0.80	1.20
9	3′-NO_2	−0.25	−0.04	0.38	−0.42	0.71	0.08
10	4′-NO_2	−0.25	−0.02	0.32	−0.34	0.78	0.08
12	4′-OH	−0.36	−0.38	0.44	−0.82	−0.37	0.08
13	3′-NH_2	−0.94	−0.60	−1.25	0.65	−0.16	0.08
14	4′-NH_2	−0.94	−0.61	0.32	−0.93	−0.66	0.08
16	3′-OCH_3	0.06	0.14	0.40	−0.26	0.12	0.08
17	4′-OCH_3	0.06	0.14	0.63	−0.49	−0.27	0.08
18	2′-F	−0.06	0.03	−0.29	0.32	0.16	0.36
19	4′-F	0.14	0.03	−0.36	0.39	0.06	0.08
20	2′-Cl	0.46	0.08	−0.90	0.98	0.25	1.07
21	4′-Cl	0.71	0.40	0.48	−0.08	0.23	0.08
23	4′-CF_3	0.88	0.58	0.40	0.18	0.54	0.08

and selectivity, and when combined with previous results,[11] leads to a broader understanding of the main factors eliciting MAO inhibitory activity and selectivity of condensed pyridazines and pyrimidines (Figure 2). Thus, the diazine and condensed C ring affect both MAO-A/B selectivity and inhibitory potency, whereas substituents on the diazine ring affect only the latter.

QSAR Analysis. For X-phenyl derivatives of IPyd, a previous QSAR model[11b] related MAO-B inhibition mostly to lipophilic and electronic properties of substituents and to a steric negative effect of ortho substituents. A small contribution had been also noted for the volume of para substituents. Using the RP-HPLC-derived lipophilic substituent constants and the novel thermodynamic parameters derived from RP-HPLC retention offered an opportunity to examine the capacity of these chromatographic descriptors to account for lipophilic interactions in enzyme−inhibitor complexes. Separate enthalpy or entropy parameters rather than free energy parameters may improve the correlation coefficient in some QSAR equations, e.g., blood−brain barrier permeation.[23] In this study, group contribution toward retention, in analogy with substituent extrathermodynamic parameters (e.g., the Hansch π constant), can be defined as

$$\tau = \log k_{R-X} - \log k_{R-H} = -(\Delta(\Delta G°)_X)/2.303RT$$

$$= -(\Delta(\Delta H°)_X)/2.303RT + (\Delta(\Delta S°)_X)/R \qquad (3)$$

When enthalpic and entropic contributions to retention are represented as τ_H and τ_S, respectively, one obtains

$$\tau = \tau_H + \tau_S \qquad (4)$$

$$\tau_H = -(\Delta(\Delta H°)_X)/2.303RT \qquad (5)$$

$$\tau_S = (\Delta(\Delta S°)_X)/R \qquad (6)$$

Using eqs 3, 5, and 6, we calculated τ, τ_H, and τ_S for the subset of 3-phenyl-5*H*-indeno[1,2-*c*]pyridazin-5-ones (**7**−**23**) listed in Table 3. The QSAR results of 3-(X-Ph) IPyd are shown in Table 4, whereas the squared correlation matrix of variables is shown in Table 5. The chromatographic substituent constant τ (which alone explains about 55% of the *y*-variance, eq 8) is here a better parameter than other lipophilicity descriptors. Due to a high intercorrelation, τ_H and τ_S cannot be used together in a regression equation. To improve the equation ($r^2 > 0.80$), the electronic σ constant and the volume descriptor of ortho substituents ($V_{W(2')}$), taken from standard compilations,[16] also had to be included (eqs 9−10). Thus, electronic properties and steric effects represent additional factors modulating MAO-B inhibition. Actually, the importance of hydrophobic interactions with a hydrophobic site and electronic interactions with a nucleophilic site of the enzyme had been postulated by others[24] on the basis of results from univariate regression analysis carried out on sets of various heterocyclic MAO-B inhibitors. The results of our QSAR study, consistent with these models, contribute to a better definition of the nature of the forces responsible for reversible inhibition of MAO-B and are in good agreement with a recently published model of reversible inhibition of MAO-B by diazo heterocyclic compounds.[25] This model shows that lipophilicity is the most important parameter governing binding to the MAO-B inhibition site, whereas minor roles are played by conformation (i.e., planar conformations are preferred) and hydrogen bonding.

Conclusions

Two main conclusions emerge from the activities of diazine derivatives as MAO inhibitors. First, structure−activity relationships of the derivatives synthesized and tested to date unravel the main factors affecting inhibitory activity and selectivity toward MAO-A and MAO-B. Thus, most of the condensed pyridazines are reversible MAO-B inhibitors, with no or little effect on MAO-A, whereas the condensed pyrimidines prove to be reversible inhibitors endowed with an appreciable selectivity toward MAO-A. Substituents on the diazine nucleus modulate the inhibitory activity. In contrast, the nature of the ring(s) condensed with diazine appear to affect significantly the selectivity toward MAO-A and MAO-B.

Second, the QSAR results reported in this paper bring further evidence that lipophilicity is a property that significantly modulates MAO-B but not MAO-A inhibition. Multiple linear regression analysis yielded QSAR models showing the importance of lipophilic, electronic, and steric properties of indenopyridazines in determining MAO-B inhibition. In contrast, any attempt to derive quantitative models for MAO-A inhibition was inconclusive, at least within the examined property space. This is compatible with the known mechanism of reversible inhibition of MAO-A where the formation of the complex between the inhibitor and the FAD cofactor appears as a crucial event.[26] This implies electrostatic interactions and charge-transfer bonding as the major contributions to the stability of the FAD−inhibitor complex. Work is in progress in our laboratory, using chromatography-based model systems and quantum chemical calculations to find suitable electrostatic descriptors.

Experimental Section

Chemistry. Melting points were determined by the capillary method on a Gallekamp MFB 595 010M electrothermal apparatus and are uncorrected. Elemental analyses were performed on a Carlo Erba 1106 analyzer; for C, H, and N, the results agreed to within ±0.40% of the theoretical values.

Table 4. QSAR of 3-(X-Phenyl)-5*H*-indeno[1,2-*c*]pyridazin-5-one MAO-B Inhibitors[a] ($n = 14$, Table 3) Using Lipophilicity and Other Physical Parameters

eq no.	QSAR eqs	r^2	q^2	s	F
7	$pIC_{50} = 0.96(\pm0.39)\pi + 5.43(\pm20)$	0.333	0.131	0.738	5.998
8	$pIC_{50} = 1.84(\pm0.48)\tau + 5.48(\pm16)$	0.555	0.437	0.603	14.94
9	$pIC_{50} = 0.78(\pm0.24)\pi + 0.94(\pm0.30)\sigma - 1.67(\pm0.32)V_{W(2')} + 5.70(\pm0.14)$	0.830	0.687	0.408	16.26
10	$pIC_{50} = 1.20(\pm0.38)\tau + 0.84(\pm0.32)\sigma - 1.31(\pm0.35)V_{W(2')} + 5.64(\pm0.14)$	0.821	0.704	0.419	15.27

[a] Only compounds with measurable IC_{50} values were included in the regression analysis (i.e., **7**−**10**, **12**−**14**, **16**−**21**, and **23**).

Table 5. Squared Correlation Matrix of Variables Used in QSAR Analysis

	pIC_{50}	π	τ	τ_H	τ_S	σ	$Vw(2')$
pIC_{50}	1	0.333	0.555	0.374	0.049	0.152	0.258
π		1	0.863	0.064	0.086	0.157	0.012
τ			1	0.206	0.013	0.139	0.031
τ_H				1	0.696	0.020	0.436
τ_S					1	0.151	0.394
σ						1	0.137
$V_{w(2')}$							1

IR spectra were recorded using potassium bromide disks on a Perkin-Elmer 1600 FT-IR spectrophotometer. Only the most significant IR absorption bands are listed. ^{1}H NMR spectra were recorded at 300 MHz on a Bruker 300 instrument. Chemical shifts are expressed in δ (ppm) and the coupling constants J in hertz (Hz). The following abbreviations are used, s, singlet; d, doublet; t, triplet; q, quartet; qn, quintet; m, multiplet; dd, double doublet; br, broad signal. Signals due to OH and NH protons were located by deuterium exchange with D_2O.

4-Benzoylpyridazine (**1**) was synthesized according to the procedure described by Heinisch et al.[13] The synthesis of compounds **2**−**23** was described by Kneubühler et al.[11] and Carotti et al.[15] A pure sample of 3-Phenyl-5*H*-pyridazino[4,3-*b*]indole **32** was kindly provided by Prof. F. Campagna (University of Bari, Italy).

3-Phenyl-6,7-dihydro-5*H*-cyclopenta[*c*]pyridazine (26). A mixture of ω-bromoacetophenone (4.98 g, 25 mmol) and 4-(1-cyclopenten-1-yl)morpholine (4.2 mL, 26.25 mmol) in 50 mL of anhydrous dioxane was heated at reflux under magnetic stirring for 15 h. After the mixture cooled to 60 °C, 100 mL of 0.01 N HCl was added, and the solution was stirred at the same temperature for 2 h. After the solution cooled to room temperature, dioxane was evaporated under reduced pressure and the solution extracted with $CHCl_3$. The extracts were dried over Na_2SO_4 and evaporated to dryness. The oil residue was purified by column chromatography on silica gel (hexane/ethyl acetate, 65/35 v/v, as eluent) giving pure 2-phenacylpentan-1-one **24** (2.88 g, 57% yield). Analytical data are consistent with those reported in the literature.[27] Hydrazine hydrate 98% (0.66 mL, 13.65 mmol) was added under magnetic stirring to the solution of **24** (2.63 g, 13 mmol) in 260 mL of a solvent mixture ($CHCl_3/Et_2O$, 4/1, v/v). After 4 h, the reaction mixture was evaporated to dryness and the oil residue so obtained was treated with Et_2O to give the intermediate **25** (not isolated), which spontaneously dehydrogenated to **26**. Pure **26** was obtained in 58% yield by column chromatography on silica gel ($CHCl_3$/AcOEt, 9/1 v/v, as eluent): mp 124−5 °C, from $CHCl_3$/hexane; ^{1}H NMR ($CDCl_3$) δ 8.00 (dd, 2H, $J = 7.9, 1.5$), 7.65 (t, 1H, $J = 1.2$), 7.52−7.44 (m, 3H), 3.25 (t, 2H, $J = 7.6$), 3.02 (td, 2H, $J = 7.6, 1.2$), 2.19 (qn, 2H, $J = 7.6$); IR (cm^{-1}) 1415, 695. Anal. ($C_{13}H_{12}N_2$) C, H, N.

5,6,7,8-Tetrahydrocinnolin-5-one (29). The intermediate triketone **27** was prepared by the reaction between cyclohexan-1,3-dione and 2-bromoacetophenone, according to the procedure described by Stetter[14] and used without further purification (mp 146−8 °C; lit. mp 158.5 °C) for the subsequent reaction. Hydrazine hydrate 98% (0.97 mL, 2 mmol) was added under magnetic stirring to a solution of **27** (0.46 g, 2 mmol) in 40 mL of anhydrous EtOH. After 30 min, 0.45 g (2 mmol) of 2,3-dichloro-5,6-dicyano-1,4-benzoquinone (DDQ) was added, and the solution was heated at reflux for 30 min and then evaporated to dryness to give an oil residue. The oil was treated with $CHCl_3$ and the solid filtered off. The chloroform solution was evaporated to dryness, and the solid residue was purified by crystallization to give **29** (0.35 g, 78% yield): mp 108−9 °C, from $CHCl_3$/hexane; ^{1}H NMR ($CDCl_3$) δ 8.24 (s, 1H), 8.12 (dd, 2H, $J = 7.8, 1.9$), 7.56−7.46 (m, 3H), 3.42 (t, 2H, $J = 6.2$), 2.78 (t, 2H, $J = 6.6$), 2.28 (qn, 2H, $J = 6.4$); IR (cm^{-1}) 1700, 1405. Anal. ($C_{14}H_{12}N_2O$) C, H, N.

3-Phenyl-5,6,7,8-tetrahydropyrimido[4,5-*c*]pyridazin-5,7-dione (30). A solution of alloxan monohydrate (0.32 g, 2 mmol) and acetophenone (0.23 mL, 2 mmol) in 4 mL of glacial AcOH was heated at reflux for 2.5 h. The reaction mixture was allowed to cool to room temperature, and then 0.15 mL (3 mmol) of hydrazine hydrate (98%) was added. After stirring overnight, the reaction mixture was filtered off, and the solution was evaporated to dryness. The resulting yellow oil residue was treated with ethyl acetate to give crystals of compound **30** (0.20 g, 76% yield): mp 271−2 °C, from dioxane; ^{1}H NMR (DMSO-d_6) δ 14.30 (br, 1H), 11.46 (br, 1H), 8.65 (s, 1H), 7.99−7.94 (m, 2H), 7.81 (br, 1H), 7.68 (br, 1H), 7.60−7.53 (m, 3H); IR (cm^{-1}) 1690, 1570, 1375. Anal. ($C_{12}H_{10}N_4O_3$) C, H, N.

3-(4′-Trifluoromethylphenyl)-5,6,7,8-tetrahydropyrimido[4,5-*c*]pyridazin-5,7-dione (31). Compound **31** was prepared in 85% yield by the same procedure described for **30**: mp 274−6 °C dec, from EtOH/dioxane; ^{1}H NMR (acetone-d_6) δ 8.81 (s, 1H), 8.24 (d, 1H, $J = 8.0$), 7.97 (br, 1H), 7.89 (d, 1H, $J = 8.0$), 6.68 (br, 1H), 7.60−7.53 (m, 2H); IR (cm^{-1}) 1720, 1335, 1120. Anal. ($C_{13}H_7F_3N_4O_2$) C, H, N.

1-(*N*,*N*-dimethylaminomethyliden)indan-2-one (33a). To a solution of indan-2-one (2.64 g, 20 mmol) in 40 mL of $CHCl_3$ was added dropwise 2.65 mL (20 mmol) of *N*,*N*-dimethylformamide dimethyl acetal under magnetic stirring at room temperature. Then the solvent was evaporated under reduced pressure, and the enaminone **33a** was obtained as violet solid (2.70 g, yield 72%) and used without further purification for the subsequent reaction: mp 86−8 °C dec, from $CHCl_3$/hexane; ^{1}H NMR ($CDCl_3$) δ 7.25 (t, 1H, $J = 7.7$), 7.15 (d, 1H, $J = 7.7$), 7.14 (t, 1H, $J = 7.7$), 6.99 (d, 1H, $J = 7.7$), 6.95 (s, 1H), 3.39 (d, 1H, $J = 14.0$), 3.36 (d, 1H, $J = 14.0$), 3.33 (s, 3H), 3.23 (s, 3H); IR (cm^{-1}) 1670, 1380, 755. Anal. ($C_{12}H_{13}NO$) C, H, N.

2-Phenyl-9*H*-indeno[2,1-*d*]pyrimidine (34a). To a suspension of sodium methoxide (0.162 g, 3 mmol) and benzamidine hydrochloride hydrate (0.57 g, 3 mmol) in 3 mL of anhydrous EtOH were added dropwise under stirring 3 mL of a solution of enaminone **33a** (0.28 g, 1.5 mmol) in anhydrous EtOH. The reaction mixture was refluxed for 1 h, and then it was allowed to cool, filtered off, poured into 30 mL of water, and neutralized with 1 N HCl. The aqueous solution was extracted with $CHCl_3$, and the extracts were dried over Na_2SO_4 and evaporated to dryness giving a violet solid residue (0.36 g, 99% yield) of 2-Phenyl-9*H*-indeno[2,1-*d*]pyrimidine (**34a**), which was partly purified by treatment with activated carbon and crystallized from EtOH: mp 185−6 °C, from EtOH; ^{1}H NMR ($CDCl_3$) δ 9.10 (s, 1H), 8.54−8.46 (m, 2H), 7.84 (dd, 1H, $J = 6.2, 2.1$), 7.61 (dd, 1H, $J = 7.1, 1.1$), 7.53−7.37 (m, 5H), 4.06 (s, 2H); IR (cm^{-1}) 1550, 1385, 755, 710, 690. Anal. ($C_{17}H_{12}N_2$) C, H, N.

2-Phenyl-9*H*-indeno[2,1-*d*]pyrimidin-9-one (35). A solution of **34a** (0.73 g, 0.3 mmol) and chromic anhydride (0.40 g, 0.4 mmol) in 6 mL of glacial acetic acid was heated at reflux for 30 min. Upon cooling to room temperature, the solution was diluted with 20 mL of water and extracted with $CHCl_3$. The combined extracts were washed with a saturated solution

of $NaHCO_3$ and water and then dried (Na_2SO_4) and evaporated to dryness. The oil residue obtained was purified by flash chromatography on silica gel, using $CHCl_3$/hexane (9/1, v/v) as eluent, to give 0.39 g of compound **35**, which was further purified by crystallization from EtOH (50% yield): mp 228−9 °C, from ethanol; ^{1}H NMR ($CDCl_3$) δ 9.07 (s, 1H), 8.55−8.50 (m, 2H), 7.81 (dt, 1H, J = 7.4, 1.0), 7.67−7.59 (m, 2H), 7.52−7.47 (m, 3H), 7.43 (td, 1H, J = 7.1, 1.8); IR(cm^{-1}) 1730, 1385. Anal. ($C_{17}H_{10}N_2O$) C, H, N.

2-(*N*,*N*-dimethylaminomethyliden)indan-1-one (33b). A mixture of 0.66 g (5.0 mmol) of indan-1-one and 1.25 mL (9.4 mmol) of *N*,*N*-dimethylformamide dimethyl acetal was heated at reflux for 3 h. Upon cooling to room temperature, the enaminone **33b** precipitated as a red orange solid and was collected by filtration (0.92 g, yield 98%) and used without further purification for the subsequent reaction (mp 148−50 °C; lit.[28] mp 158 °C, from $CHCl_3$/hexane).

2-Phenyl-5*H*-indeno[1,2-*d*]pyrimidine (34b). With the exception of reaction time (7h at reflux), this compound was prepared in 52% yield following the procedure described above for compound **34a**: mp 155−6 °C, from EtOH; ^{1}H NMR ($CDCl_3$) δ 8.89 (s, 1H), 8.56 (dd, 2H, J = 8.1, 1.6), 8.26 (dd, 1H, J = 6.3, 2.4), 7.66−7.61 (m, 1H), 7.57−7.44 (m, 5H), 3.95 (s, 2H); IR(cm^{-1}) 1580, 1545, 1385, 745. Anal. ($C_{17}H_{12}N_2$) C, H, N.

2-Phenyl-5*H*-indeno[1,2-*d*]pyrimidin-5-one (36). The oxidation of compound **34b** by CrO_3 to give compound **36** was carried out following the same procedure described for compound **35** (reaction time, 4 h; 87% yield): mp 172−3 °C, from EtOH; ^{1}H NMR ($CDCl_3$) δ 8.94 (s, 1H), 8.60 (dd, 2H, J = 8.0, 1.7), 8.05 (d, 1H, J = 7.4), 7.69 (td, 1H, J = 7.4, 1.0), 7.60 (dd, 1H, J = 7.4, 1.0), 7.56−7.50 (m, 3H), 7.44 (t, 1H, J = 7.4); IR (cm$_{-1}$) 1720, 1390, 740. Anal. ($C_{17}H_{10}N_2O$) C, H, N.

Determination of Partition Coefficients. Partition coefficients were determined in 1-octanol (P_{oct}) or cyclohexane (P_{cyh}) and pH 7.4 phosphate buffer (0.05 M) at room temperature by a conventional shake-flask technique. Solute concentrations in aqueous phase before partitioning were within the range 1×10^{-4} to 1×10^{-3} M. To help dissolution of very hydrophobic solutes in water, methanol or *N*,*N*-dimethylformamide was used in a small volume (less than 2% v/v). The concentration of each compound in the aqueous phase before and after partitioning was measured spectrophotometrically (UV) or by HPLC. All of the partition coefficients are the means of at least five determinations within the above concentration range.

Calculated log P_{oct} values were obtained by the fragmental method of Hansch and Leo[16] using the MacLog P 2.0 program (BioByte Corp., Claremont, CA).

Thermodynamics of Retention in RP-HPLC. All chromatographic measurements were performed on a Waters HPLC model 600 multisolvent delivery system (Waters Assoc., Milford, MA) equipped with a Waters 481 variable wavelength detector. The mobile phase, which constisted of a mixture of methanol and 0.01 M phosphate buffer, pH 5.6 (45/55, v/v), was continually purged with helium. A 5-μm Supelcosil LC-18 column (50 × 4.6 mm i.d.; Supelco Inc., Bellefonte, PA) was used as the stationary phase. The mobile phase was delivered from a glass reservoir, which was thermostated at the same temperature as that of the column. Temperature control, ±0.1 °C, was mantained by a recirculating water bath.

The chromatographic parameters were averages of at least triplicate determinations of each solute, and detection was at 254 or 210 nm. Retention data were measured at seven different temperatures over a temperature range 18 to 48 °C. Before each run, the column was equilibrated with mobile phase for at least 30 min at a flow rate of 1.0 mL/min. This procedure was repeated each time the column temperature was changed. The column void time, t_0, was determined by recording the first baseline perturbation. The capacity factor k for each solute was calculated as

$$k = (t_R - t_0)/t_0 \quad (11)$$

where t_R is the average retention time of triplicate injections of the analyte.

The enthalpy and entropy of retention were derived from a van't Hoff plot. In each experimental plot the squared correlation coefficient usually amounted to about 0.95. Moreover, thermodynamic data were examined for enthalpy−entropy compensation effects.[20] An enthalpy−entropy compensation in RP-HPLC exists when the following relatioship is verified

$$\ln k_T = -(\Delta H°/R)(1/T - 1/\beta) - \Delta G_\beta/R\beta + \ln \phi \quad (12)$$

where β is a compensation proportionality factor between $\Delta H°$ and $\Delta S°$; this factor has the dimension of absolute temperature and is generally termed the compensation temperature. Since in our study both enthalpy and entropy were derived from the same equation (van't Hoff equation), to distinguish between artifactual and genuine chemical compensation effect, we applied the method proposed by Krug et al.[29] to the analysis of our data. Thus, in the plot of ln k vs $\Delta H°$ at T_{hm} (see Figure 3), from the slope of the line relative to IPyd congeners (**12** and **14** omitted as outliers; n = 22; r^2 = 0.806; s = 0.512), we calculated β = 592 K with a 95% confidence interval of 495−738 K and compared it with the harmonic mean temperature, T_{hm} (306 K). Since T_{hm} did not fall within the 95% confidence interval of the estimated value for β, we could conclude that the observed compensation has a chemical cause.

X-ray Crystallography of $C_{17}H_9N_3O_3$ (8). Crystal data for $C_{17}H_9N_3O_3$: very thin orange plates from ethanol, 0.84 × 0.42 × 0.04 mm, triclinic, space group $P\bar{1}$ (No. 2), a = 7.888(3), b = 8.973(3), c = 11.565 Å, α =105.08(2)°, β = 99.57(2)°, γ = 113.10(2)°, V = 693.0(4) Å, Z = 2, fw 303.27, d_{calc} = 1.453 g/cm^3, μ(Mo Kα) = 0.103 mm^{-1}. Data were collected at room temperature (293 K) on a Stoe AED2 4-circle diffractometer using Mo Kα graphite monochromated radiation (λ = 0.710 73 Å) with $\omega/2\theta$ scans in the 2θ range 5−51°. A total of 2400 independent reflections were measured, only 847 could be observed with $I > 2\sigma(I)$, limits h −9/9, k −10/10, l 0/13, and no correction for absorption was applied. The structure was solved by direct methods using the program SHELXS-86.[30] The refinement and all further calculations were carried out using SHELXL-93.[31] All of the H-atoms were included in calculated positions and allowed to ride on the corresponding C atom. The non-H atoms were refined anisotropically, using weighted full-matrix least-squares on F^2. Final R_1 = 0.0883, R_{w2} = 0.1989 (observed data), goodness of fit on F^2 0.920, residual density max/min 0.256/−0.252 e Å^{-3}. The data-to-parameter ratio (847/209) for the observed data was only 4.1 due to the fact that the crystal did not diffract significantly beyond 40° in 2θ.

The bond lengths and angles are normal within experimental error. The molecular structure and crystallographic numbering scheme of **8** is illustrated in Figure 2, drawn using the program Xtal_GX.[32] Full tables of atomic parameters and bond lengths and angles may be obtained from the Cambridge Crystallographic Data Centre, 12 Union Road, Cambridge CB2 1EZ (UK) on quoting the full journal citation.

Preparation of Rat Brain Mitochondria. Rat brain mitochondria were isolated according to the method of Clark[33] modified by Walther et al.[34] For further details, see Thull et al.[35] The protein content of the washed mitochondrial fraction was determined according to the procedure of Lowry[36] with bovine serum albumin as a standard.

MAO Inhibition Assay. The method of Weissbach[21] was modified to measure inhibitory activities. IC_{50} values were calculated from a hyperbolic equation described elsewhere.[35] Time dependence was tested by preincubating for 5 and 15 min at 37 °C and at a single concentration of the inhibitor. Reversibility was demonstrated by measuring the degree of inhibition in the presence of a higher substrate concentration (540 μM). For details on the MAO assay, see Kneubühler et al.[11]

Regression Analysis. Multiple linear regression (MLR) analysis was performed using the commercially available statistical package PARVUS 1.2[37] running on an IBM-compatible PC.

Acknowledgment. The Italian authors gratefully acknowledge support from MURST and CNR (Rome, Italy). B.T. and P.A.C. are indebted to the Swiss National Science Foundation for support. The authors wish to thank Prof. F. Campagna (University of Bari, Italy) for the kind gift of a pure sample of 3-phenyl-5*H*-pyridazino[4,3-*b*]indole.

Supporting Information Available: Tables of relevant details of the X-ray crystallographic studies and tables of final atomic parameters, full bond lengths and angles, anisotropic thermal parameters, hydrogen atom positions, selected torsion angles, and various least-squares planes (7 pages). Ordering information is given on any current masthead page.

References

(1) Tipton, K. F. Enzymology of monoamine oxidase. *Cell Biochem. Funct.* **1986**, *4*, 79−87.

(2) Kalgutkar, A. S.; Castagnoli, N., Jr.; Testa, B. Selective inhibitors of monoamine oxidase (MAO-A and MAO-B) as probes of its catalytic site and mechanism. *Med. Res. Rev.* **1995**, *15*, 325−388.

(3) (a) Bach, A. W. J.; Lan, N. C.; Johnson, D. L.; Abell, C. W.; Bembenek, M. E.; Kwan, S. W.; Seeburg, P. H.; Shih, J. C. cDNA cloning of human liver monoamine oxidase A and B: Molecular basis of differences in enzymatic properties. *Proc. Natl. Acad. Sci. U.S.A.* **1988**, *85*, 4934−4938. (b) Grimsby, J.; Chen, K.; Wang, L. J.; Lan, N. C.; Shih, J. C. Molecular basis of human MAO A and B. *Proc. Natl. Acad. Sci. U.S.A.* **1991**, *88*, 3637−3641.

(4) (a) Wu, H.-F.; Chen, K.; Shih, J. C. Site-directed mutagenesis of monoamine oxidase A and B: role of cysteines. *Mol. Pharmacol.* **1993**, *43*, 888−893. (b) Zhong, B.; Silverman, R. B. Identification of the active site cysteine in bovine liver monoamine oxidase B. *J. Am. Chem. Soc.* **1997**, *119*, 6690−6691. (c) Tsugeno, Y.; Ito, A.; A key amino acid responsible for substrate selectivity of monoamine oxidase A and B. *J. Biol. Chem.* **1997**, *272*, 14033−14036.

(5) Langston, J. W.; Ballard, P.; Tetrud, J. W.; Irwin, I. Chronic parkinsonism in humans due to a product of meperidine-analog synthesis. *Science* **1983**, *219*, 979−980.

(6) Strolin-Benedetti, M.; Dostert, P. L. Monoamine oxidase: From physiology and pathophysiology to the design and clinical application of reversible inhibitors. In *Advances in Drug Research*; Testa, B., Ed.; Academic Press: London, U.K., 1992; Vol. 23, pp 65−125.

(7) (a) Allain, H.; Bentué-Ferrer, D.; Belliard, S.; Derousné, C. Pharmacology of Alzheimer's disease. In *Progress in Medicinal Chemistry*; Ellis, C. P., Luscombe, D. K., Eds; Elsevier Science: Amsterdam, NL, 1997; Vol. 34, pp 1−67. (b) Freedman, M.; Rewilak, D.; Xerri, T.; Cohen, S.; Gordon, A. S.; Shandling, M.; Logan, A. G. L-deprenyl in Alzheimer's disease: Cognitive and behavioral effects. *Neurology* **1998**, *50*, 660−668. (c) Bongioanni, P.; Mondino, C.; Boccardi, B.; Borgna, M.; Castagna. M. *Neurodegener.* **1996**, *5*, 351−357.

(8) (a) Youdim, M. B. H.; Finberg, J. P. M. New directions in monoamine oxidase A and B selective inhibitors and substrates. *Biochem. Pharmacol.* **1991**, *41*, 155−162. (b) Cesura, A. M.; Pletscher, A. The new generation of monoamine oxidase inhibitors. In *Progress in Drug Research*; Jucker, E., Ed.; Birkhäuser Verlag: Basel, Switzerland, 1992; Vol. 38, pp 171−297. (c) Da Prada, M.; Kettler, R.; Keller, H. H.; Cesura, A. M.; Richards, J. G.; Saura Marti, J.; Muggli-Maniglio, D.; Wyss, P. C.; Kyburz, E.; Imhof, R. From moclobemide to Ro 19-6327 and Ro 41-1049: The development of a new class of reversible, selective MAO-A and MAO-B inhibitors. *J. Neural Transm.* [*Suppl.*] **1990**, *29*, 279−292.

(9) Altomare, C.; Carrupt, P.-A.; Gaillard, P.; El Tayar, N.; Testa, B.; Carotti, A. Quantitative structure-metabolism relationship analyses of MAO-mediated toxication of 1-methyl-4-phenyl-1,2,3,6-tetrahydropyridine and analogues. *Chem. Res. Toxicol.* **1992**, *5*, 366−375.

(10) Thull, U.; Kneubühler, S.; Gaillard, P.; Carrupt, P.-A.; Testa, B.; Altomare, C.; Carotti, A.; Jenner, P.; McNaught, K. St. P. Inhibition of monoamine oxidase by isoquinoline derivatives: Qualitative and 3D-quantitative structure-activity relationships. *Biochem. Pharmacol.* **1995**, *50*, 869−877.

(11) (a) Kneubühler, S.; Carta, V.; Altomare, C.; Carotti, A.; Testa, B. Synthesis and monoamine oxidase inhibitory activity of 3-substituted 5*H*-indeno[1,2-*c*]pyridazines. *Helv. Chim. Acta* **1993**, *76*, 1954−1963. (b) Kneubühler, S.; Thull, U.; Altomare, C.; Carta, V.; Gaillard, P.; Carrupt, P.-A.; Carotti, A.; Testa, B. Inhibition of monoamine oxidase-B by 5*H*-indeno[1,2-*c*]pyridazines: Biological activities, quantitative structure-activity relationships (QSARs) and 3D-QSARs. *J. Med. Chem.* **1995**, *38*, 3874−3883.

(12) Gaillard, P.; Carrupt, P.-A.; Testa, B.; Boudon, A. Molecular lipophilicity potential, a tool in 3D QSAR: Method and applications. *J. Comput.-Aided Mol. Des.* **1994**, *8*, 83−96.

(13) Heinish, G.; Jentzsch, A.; Pailer, M. C-4 Substituted pyridazines by homolitic alkylation and acylation. *Monatsh. Chem.* **1974**, *105*, 648−652.

(14) Stetter, H.; Siehnhold, E. Zur kenntnis des kondensationsproduktes aus dihydroresorcin und phenacylbromid. *Chem. Ber.* **1955**, *88*, 271−274.

(15) (a) Carotti, A.; Carta, V.; Campagna, F.; Altomare, C.; Casini, G.; An efficient route to biologically active 5*H*-indeno[1,2-*c*]-pyridazin-5-ones. *Farmaco* **1993**, *48*, 137−141. (b) Altomare, C.; Campagna, F.; Carta, V.; Cellamare, S.; Carotti, A.; Genchi, G.; De Sarro, G. *Farmaco* **1994**, *49*, 313−323.

(16) (a) Hansch, C.; Leo, A. The FRAGMENT method of calculating partition coefficients. In *Substituent constants for correlation analysis in chemistry and biology*. Wiley: New York, 1979; pp 18−43. (b) Hansch, C.; Leo, A.; Hoekman, D. *Exploring QSAR. Hydrophobic, Electronic, and Steric Constants*, ACS Professional Reference Book; American Chemical Society: Washington, DC, 1995. (c) Van de Waterbeemb, H.; Testa, B. The parametrization of lipophilicity and other structural properties in drug design. In *Advances in Drug Research*; Testa, B., Ed.; Academic Press: London, U.K., 1987; Vol. 16, pp 85−225.

(17) MacLog P 2.0 program. BioByte Corp., Claremont, CA.

(18) Leo, A. J. The future of log *P* calculation. In *Lipophilicity in Drug Action and Toxicology. Methods and principles in Medicinal Chemistry*; Pliska, V., Testa, B., Van de Waterbeemd, H., Eds.; VCH Verlagsgesellschaft: Weinheim, D, 1996; Vol. 4, pp 157−171.

(19) Dorsey, J. G.; Dill, K. A. The molecular mechanism of retention in reversed-phase liquid chromatography. *Chem. Rev.* **1989,** *89*, 331−346.

(20) (a) Melander, W.; Campbell, D. E.; Horvatth, Cs. Enthalpy-entropy compensation in reversed-phase chromatography. *J. Chromatogr.* **1978**, *158*, 215−225. (b) Tomlinson, E. Enthalpy-entropy compensation analysis of pharmaceutical, biochemical and biological systems. *Int. J. Pharm.* **1983**, *13*, 115−144. (c) Lumry, R.; Rajender, S. Enthalpy-entropy compensation phenomena in water solutions of proteins and small molecules: a ubiquitous property of water. *Biopolymers* **1970**, *9*, 1125−1227. (d) Tomlinson, E.; Poppe, H.; Kraak, J. C. Thermodynamics of functional groups in reversed-phase high performance liquid-solid chromatography. *Int. J. Pharm.* **1981**, *7*, 225−243. (e) Repond, C.; Mayer, J. M.; Van de Waterbeemd, H.; Testa, B.; Linert, W. Thermodynamics and mechanism of partitioning of pyridylalkanamides in *n*-octanol/water and di-*n*-butyl ether/water. *Int. J. Pharm.* **1987**, *38*, 47−57.

(21) Weissbach, H.; Smith, T. E.; Daly, J. W.; Witkop, B.; Udenfriend, S. A rapid spectrophotometric assay of monoamine oxidase based on the rate of disappearance of kynuramine. *J. Biol. Chem.* **1960**, *235*, 1160−1163.

(22) Thull, U.; Testa, B. Screening of unsubstituted cyclic compounds as inhibitors of monoamine oxidases. *Biochem. Pharmacol.* **1994**, *47*, 2307−2310.

(23) (a) Da, Y.-Z.; Ito, K.; Fujiwara, H. Energy aspects of oil/water partition leading to the novel hydrophobic parameters for the analysis of quantitative structure-activity relationships. *J. Med. Chem.* **1992**, *35*, 3382−3387. (b) Da, Y.-Z., Yanagi, J.; Tanaka, K.; Fujiwara, H. Termochemical aspects of partition. Quantitative structure-activity relationships of benzyldimethylalkylammonium chlorides. *Chem. Pharm. Bull.* **1993**, *41*, 227−230. (c) Kai, J.; Nakamura, K.; Masuda, T.; Ueda, I.; Fujiwara, H. Thermodynamic aspects of hydrophobicity and the blood-brain barrier permeability studied with a gel filtration chromatography. *J. Med. Chem.* **1996**, *39*, 2621−2624.

(24) (a) Mazouz, F.; Lebreton, L.; Milcent, R.; Burstein, C. Inhibition of monoamine oxidase types A and B by 2-aryl-4*H*-1,3,4-oxadiazin-5(6*H*)-one derivatives. *Eur. J. Med. Chem.* **1988**, *23*, 441−451. (b) Mazouz, F.; Lebreton, L.; Milcent, R.; Burstein, C. 5-Aryl-1,3,4-oxadiazol-2(3*H*)-one derivatives and sulfur analogues as new selective and competitive monoamine oxidase type B inhibitors. *Eur. J. Med. Chem.* **1990**, *25*, 659−671. (c) Castelli, F.; Pignatello. R.; Sarpietro, M. G.; Mazzone, P.; Raciti, G.; Mazzone, G. Correlation between monoamino oxidase inhibitor activity of some thiazol-2-ylhydrazines and their interaction with dipalmitoylphopsphatidilcoline liposomes. *J. Pharm. Sci.* **1994**, *83*, 362−366.

(25) Wouters, J.; Ooms, F.; Jegham, S.; Koenig, J. J.; George, P.; Durant, F. Reversible inhibition of type B monoamine oxidase. Theoretical study of model diazo heterocyclic compounds. *Eur. J. Med. Chem.* **1997**, *32*, 721−730.
(26) (a) Moureau, F.; Wouters, J.; Vercauteren, D. P.; Collin, S.; Evrad, G.; Durant, F.; Ducrey, F.; Koenig, J. J.; Jarreau, F. X. A reversible monoamine oxidase inhibitor, Toloxatone: Spectrophotometric and molecular orbital studies of the interaction with flavin adenine dinucleotide (FAD). *Eur. J. Med. Chem.* **1994**, *29*, 269−277. (b) Moureau, F.; Wouters, J.; Depas, M.; Vercauteren, D. P.; Durant, F.; Ducrey, F.; Koenig, J. J.; Jarreau, F. X. A reversible monoamine oxidase inhibitor, Toloxatone: Comparison of its physicochemical properties with those of other inhibitors including Brofaromine, Harmine, R40519 and Moclobemide. *Eur. J. Med. Chem.* **1995**, *30*, 823−838.
(27) Stetter, H.; Halse, W. Addition of aldehydes to cyclic α-methylene ketones. *Chem. Ber.* **1984**, *117*, 682−693.
(28) Wagner, R. M.; Jutz, C. A variance of the pyrimidine synthesis. *Chem. Ber.* **1971**, *104*, 2975−2983.
(29) Krug, R. R.; Hunter, W. G., Grieger, R. A. Enthalpy-entropy compensation. 2. Separation of the chemical from the statistical effects. *J. Phys. Chem.* **1976**, *80*, 2341−2351.
(30) Sheldrick, G. M. SHELXS-86 Program for Crystal Structure Determination. *Acta Crystallogr.* **1990**, *A46*, 467−473.
(31) Sheldrick, G. M. SHELXL-93, Universität Göttingen, Göttingen, Germany.
(32) Hall, S. R.; du Boulay, D. Xtal_GX, Editors. University of Western Australia, Australia.
(33) Clark, J. B.; Nicklas, W. J. The metabolism of rat brain mitochondria. *J. Biol. Chem.* **1970**, *245*, 4724−4731.
(34) Walther, B.; Ghersi-Egea, J.; Minn, A.; Siest, G. Brain mitochondrial cytochrome P-450scc: Spectral and catalytic properties. *Arch. Biochem. Biophys.* **1987**, *254*, 592−596.
(35) Thull, U.; Kneubühler, S.; Testa, B.; Borges, M. F. M.; Pinto, M. M. M. Substituted xanthones as selective and reversible monoamine oxidase A (MAO-A) inhibitors. *Pharm. Res.* **1993**, *10*, 1187−1190.
(36) Lowry, O.; Rosebrough, N.; Lewis Farr, A.; Randall, R. Protein measurement with the folin phenol reagent. *J. Biol. Chem.* **1951**, *193*, 265−275.
(37) Forina, M.; Leardi, R.; Armanino, C.; Lanteri, S.; Conti, P.; Princi, P. *Parvus: an Extendable Package of Programs for Data Exploration, Classification and Correlation*; Elsevier Scientific Software: Amsterdam, 1988.

JM981005Y